Fluorescence Quenching by Oxygen of 9,10-Dimethylanthracene in Liquid and Supercritical Carbon Dioxide

Masami Okamoto* and Oh Wada

Faculty of Engineering and Design, Kyoto Institute of Technology, Matsugasaki, Sakyo-ku, Kyoto 606-8585, Japan

Fujio Tanaka

College of Integrated Arts and Sciences, Osaka Prefecture University, Gakuen-cho, Sakai 599-8531, Japan

Satoshi Hirayama

Laboratory of Physical Chemistry, Kyoto Institute of Technology, Matsugasaki, Sakyo-ku, Kyoto 606-8585, Japan

Received: August 15, 2000; In Final Form: November 9, 2000

The contribution of diffusion to the fluorescence quenching by oxygen of 9,10-dimethylanthracene (DMEA) in liquid CO_2 and supercritical CO_2 (SCF CO_2) at pressures up to 60 MPa was investigated. For comparison, the fluorescence quenching by CBr_4 of DMEA was also investigated. The apparent activation volume of the quenching rate constant, k_q, was 8 ± 1 and 10 ± 3 cm^3/mol for DMEA/O_2, and 42 ± 7 and 400 ± 90 cm^3/mol for DMEA/CBr_4 in liquid CO_2 (25 °C, 10 MPa) and SCF CO_2 (35 °C, 8.5 MPa), respectively. For DMEA/O_2, the plots of ln k_q against ln η, where η is the solvent viscosity, showed a leveling-off with decreasing the solvent viscosity, whereas for DMEA/CBr_4 they were almost linear in both liquid and SCF CO_2. The results, together with those of the pressure and the pressure-induced solvent viscosity dependences of k_q for DMEA/O_2 in *n*-alkanes (C_4 to C_7) and for DMEA/CBr_4 in *n*-hexane, revealed that the quenching competes with diffusion. The contribution of diffusion to the quenching was analyzed on the basis of a kinetic model with solvent cage in which the quenching occurs. The bimolecular rate constant for the quenching in the solvent cage, k_{bim}, was 6.0×10^{10} and 12×10^{10} M^{-1} s^{-1} in liquid CO_2 (25 °C, 10 MPa) for DMEA/O_2 and DMEA/CBr_4, respectively, and 5.7×10^{10} and 12×10^{10} M^{-1} s^{-1} in SCF CO_2 (35 °C, 8.5 MPa) for DMEA/O_2 and DMEA/CBr_4, respectively. The pressure dependence of k_{bim} and the contribution of diffusion to the quenching are discussed.

Introduction

Because of its chemical and biological importance, the quenching by oxygen of the excited states of aromatic molecules with singlet and triplet spin multiplicities has been investigated by many workers, and often concluded to be nearly or fully diffusion-controlled.[1−6] In fact, the observed quenching rate constant, k_q, for the lowest excited singlet state (S_1) of some aromatic molecules is ca. 10^{10} M^{-1} s^{-1}, which is approximately equal to the rate constant, k_{diff}, for diffusion-controlled reactions in a continuum medium with viscosity, η (in poise), calculated by the Debye equation[7,8]

$$k_{diff} = \frac{8RT}{\alpha\eta} \tag{1}$$

where α is 2000 and 3000 for the slip and stick boundary conditions, respectively. However, the discrepancy between k_q and k_{diff} thus calculated is not small. This implies that k_{diff} is not expressed by eq 1 and/or the quenching involves the additional rate processes that compete with diffusion.

Supercritical fluids (SCF), which can dissolve many compounds, are very interesting because their physical properties such as viscosity and density change dramatically with a small increase in pressure or temperature. Therefore, many types of bimolecular reactions[9−18] including fluorescence quenching have been examined in SCF as solvent. Among them, the fluorescence quenching by carbon tetrabromide (CBr_4) of some aromatic molecules that is believed to be diffusion-controlled was investigated and discussed mainly from the viewpoint of the local density augmentation and the local composition changes around the fluorophore molecules which arise as a result of the clustering of the solute molecules in SCF. For anthracene/CBr_4,[17,18] 1,2-benzanthracene/CBr_4,[18] and perylene/CBr_4[17] in SCF CO_2, the quenching was concluded to be diffusion-controlled on the basis of the fact that the viscosity dependence of k_q is similar to that predicted by eq 1. For 9-cyanoanthracene/CBr_4[17] and 9,10-diphenylanthracene/CBr_4,[17] an enhanced fluorescence quenching at near-critical CO_2 densities was observed and interpreted by the effects of the local quencher concentration augmentation.

Recently, we studied the fluorescence quenching by oxygen of 9,10-dimethylanthracene (DMEA) in *n*-alkane (C_4 to C_7) at pressures up to 400 MPa,[6] and found that the quenching constant, k_q, decreases significantly with increasing pressure. The results, together with the pressure-induced viscosity dependence of k_q, revealed that the quenching is nearly diffusion-controlled. In general, the bimolecular quenching reaction must compete with the diffusion process in a solvent with low

10.1021/jp002947t CCC: $20.00
Published on Web 12/30/2000

viscosity when the energy transfer from the S_1 state of DMEA to oxygen has a limiting rate constant. However, no evidence was found in *n*-butane ($\eta = 0.16$ cP at 25 °C and 3 MPa) that was the solvent with the lowest viscosity examined.[6] The viscosity of SCF CO_2 is very low near the critical density and increases steeply with increasing pressure. Therefore, SCF CO_2 is a suitable solvent for the study of the contribution of diffusion to the energy transfer by the collisional or exchange mechanism.

The fluorescence quenching by poly(bromoethane)s and CBr_4 of pyrene in methylcyclohexane at pressures up to 650 MPa has been examined.[19] It was found that the activation volume for k_q is negative and positive for the quenchers with low and high quenching ability, respectively. This was satisfactorily interpreted by a kinetic scheme via an encounter complex, followed by the formation of an exciplex in solvent cage, which is generally involved in the bimolecular reaction in liquid solution. The pressure dependence of the fluorescence quenching in liquid CO_2 that has very low viscosity ($\eta = 0.074$ cP at 25 °C and 10 MPa and increases monotonically with increasing pressure) may give us evidence for the competition of diffusion with the energy transfer that occurs in the solvent cage. Furthermore, the comparison with the quenching in SCF CO_2 may lead to an understanding of the solvent cage effect.

The present work is focused on the pressure and the pressure-induced solvent viscosity dependence of the fluorescence quenching by oxygen of DMEA in both liquid and SCF CO_2 in order to obtain insight into the contribution of diffusion to the collisional energy transfer from the S_1 state of DMEA to O_2. For comparison, we also studied the fluorescence quenching by CBr_4 of DMEA for which the quenching is concluded to be nearly or fully diffusion-controlled. From the results, together with data for fluorescence quenching by oxygen of DMEA in *n*-alkanes (C_4 to C_7) that was previously reported,[6] the quenching mechanism by oxygen is discussed.

Experimental Section

9,10-Dimethylanthracene (DMEA) (Aldrich Chemical Co.) was recrystallized from methanol and then purified by thin-layer chromatography. Carbon tetrabromide (CBr_4) (Wako Pure Chemicals Ltd.) of guaranteed grade was purified by sublimation twice under reduced pressure. *n*-Hexane (Merk) of spectroscopic grade and carbon dioxide (CO_2) (Sumitomo Seika; purity, 99.995%) were used as received.

Fluorescence decay curve measurements at high pressure were performed by using a 0.3 ns pulse from a PRA LN103 nitrogen laser for excitation. The fluorescence intensities were measured by a Hamamatsu R1635-02 photomultiplier through a Ritsu MC-25NP monochromator and the resulting signal was digitized by using a LeCroy 9362 digitizing oscilloscope. All data were analyzed by using a NEC 9801 microcomputer, which was interfaced to the digitizer. The associated high-pressure techniques have been described in detail elsewhere.[20]

The sample solution of DMEA in liquid and SCF CO_2 with oxygen was prepared as follows. An appropriate volume of a *n*-hexane stock solution of DMEA was placed into a high-pressure cell with four optical sapphire windows. The solvent was evaporated and the high-pressure cell was evacuated, and then filled with CO_2 from a high-pressure syringe pump (500 MPa). The oxygen concentration was determined by introducing a known pressure of synthesized air (oxygen/nitrogen/ argon = 21/78/1 vol %, Taiyo Oxygen Co.) into the high-pressure cell. The concentration of DMEA for the fluorescence lifetime measurements was less than 0.1 in absorbance (1 cm-cell) at maximum absorption wavelength in order to minimize the reabsorption effects. Sample solutions of DMEA with CBr_4 were prepared by a similar procedure. Complete dissolution of oxygen and CBr_4 in liquid and SCF CO_2 was checked by measuring the fluorescence lifetime of DMEA as a function of time.

Temperature was controlled at 25 ± 0.2 and 35 ± 0.2 °C. Pressure was measured by Nagano Keiki Seisakusho KH15 (68.6 MPa) and Minebea NS100A (49.0 MPa) strain gauges for the experiments in liquid CO_2 and SCF CO_2.

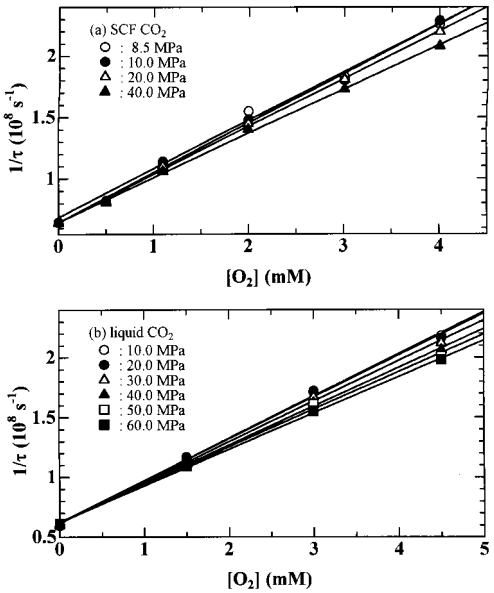

Figure 1. Plots of $1/\tau$ against the concentration of oxygen, $[O_2]$, in (a) SCF CO_2 at 35 °C and (b) liquid CO_2 at 25 °C.

Results

Fluorescence quenching was examined in the absence and presence of the quencher (Q: oxygen and CBr_4) in SCF CO_2 at 35 °C, and in liquid CO_2 and *n*-hexane at 25 °C. The decay curves were satisfactorily analyzed by a single-exponential function in all the conditions examined. The lifetimes in the absence of the quencher, τ_f^0, were found to be 16.7 ± 0.3 and 15.5 ± 0.3 ns in liquid CO_2 (25 °C, 10 MPa) and SCF CO_2 (35 °C, 8.5 MPa), respectively. They are close to those in *n*-alkanes (C_4 to C_7) and methylcyclohexane at 25 °C and 0.1 MPa (13.8−15.0 ns).[6] The lifetimes were found to be nearly independent of pressure; they were 16.1 ± 0.3 and 16.5 ± 0.3 ns at a pressure of 60 MPa in liquid CO_2 at 25 °C and SCF CO_2 at 35 °C, respectively.

The quenching rate constant, k_q, was determined using eq 2.

$$1/\tau_f - 1/\tau_f^0 = k_q[Q] \qquad (2)$$

where τ_f represents the fluorescence lifetime in the presence of the quencher. The plots of $1/\tau_f$ against the concentration of oxygen in SCF and liquid CO_2 are shown in Figure 1. Figure 2 also shows the plots of $1/\tau_f$ against the concentration of CBr_4 in SCF and liquid CO_2. The values of k_q were determined from the least-squares slopes of these plots according to eq 2, and the pressure dependence of k_q is shown in Figures 3 and 4 for DMEA/O_2 and DMEA/CBr_4, respectively. For DMEA/O_2 (Figure 3), the quenching rate constant, k_q, decreases monotonically in the whole pressure range examined, whereas for DMEA/CBr_4 (Figure 4) it steeply decreases at the lower pressure region and then gradually decreases with further increase in pressure in both liquid and SCF CO_2. The apparent activation volumes

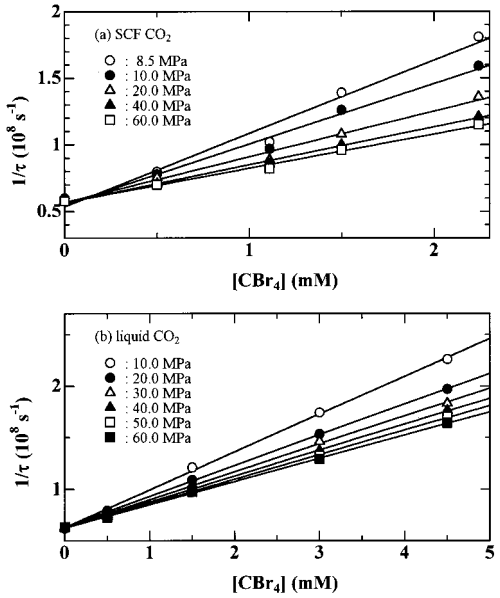

Figure 2. Plots of $1/\tau$ against the concentration of carbon tetrabromide, $[CBr_4]$, in (a) SCF CO_2 at 35 °C and (b) liquid CO_2 at 25 °C.

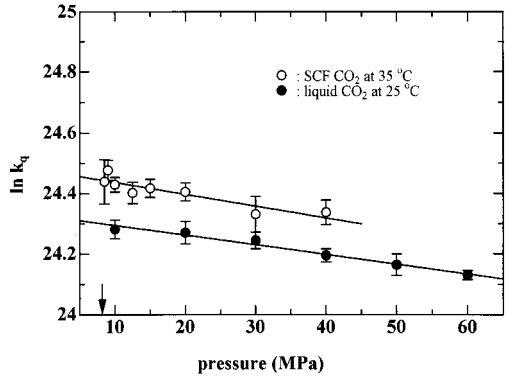

Figure 3. Pressure dependence of k_q for DMEA/O_2 in SCF CO_2 at 35 °C and liquid CO_2 at 25 °C. The solid lines were drawn by assuming that $\ln k_q = A + BP$. The arrow indicates the pressure corresponding to the critical density at 35 °C.

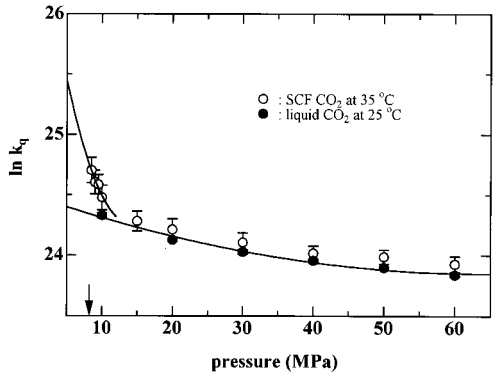

Figure 4. Pressure dependence of k_q for DMEA/CBr_4 in SCF CO_2 at 35 °C and liquid CO_2 at 25 °C. The solid lines were drawn assuming that $\ln k_q = A + BP + CP^2$. In SCF CO_2, the best-fit curve was calculated in the pressure range from 8.5 to 15 MPa. The arrow indicates the pressure corresponding to the critical density at 35 °C.

for k_q, $\Delta V_q^{\ddagger}$, evaluated by eq 3, are listed in Table 1.

$$RT(\partial \ln k_q/\partial P)_T = -\Delta V_q^{\ddagger} \qquad (3)$$

It is noted in Table 1 that $\Delta V_q^{\ddagger}$ is approximately independent of the solvents for DMEA/O_2 whereas it strongly depends on the solvents for DMEA/CBr_4. Since the fluorescence quenching by oxygen and CBr_4 of DMEA is diffusion-controlled in nature, the activation volume, $\Delta V_q^{\ddagger}$, was compared with that for the solvent viscosity, $\Delta V_\eta^{\ddagger}$, which was evaluated from the viscosity data[21−26] and is also listed in Table 1. The values of the ratio of $\Delta V_q^{\ddagger}$ to $\Delta V_\eta^{\ddagger}$ may give a crude estimate of the contribution of diffusion to the quenching; they are ca. 0.1, 0.5, and 0.01 for DMEA/O_2, and 0.5, 0.6, and 0.6 for DMEA/CBr_4 in liquid CO_2, *n*-hexane, and SCF CO_2, respectively. Thus, for DMEA/O_2 in SCF CO_2, the contribution of diffusion is small, suggesting that the quenching is nearly independent of the solvent viscosity, that is, pressure, but for the other systems examined, there is a significant contribution of diffusion to the quenching.

For the fluorescence quenching with a nearly diffusion-controlled rate, a fractional power dependence of k_q on η, which is given by eq 4, has often been observed.[5]

$$k_q = A\eta^{-\beta} \qquad (4)$$

In eq 4, A is a constant that is dependent on temperature, T, but independent of pressure, and β is less than unity. Figure 5 shows the plots of ln k_q against ln η for DMEA/O_2 in SCF CO_2 at 35 °C and liquid CO_2 at 25 °C, together with the data in *n*-alkanes (C_4 to C_7) at 25 °C.[6] The plot of ln k_q and ln η shows slightly downward curvature in liquid *n*-alkanes. The mean values of β were 0.59, 0.64, 0.71, and 0.64 in *n*-butane, *n*-pentane, *n*-hexane, and *n*-heptane, respectively, in the pressure range examined;[6] they increased to 0.74, 0.77, and 0.79 in *n*-pentane, *n*-hexane, and *n*-heptane, respectively, at pressures above 300 MPa. In liquid CO_2, the plot of ln k_q and ln η levels off with decreasing the solvent viscosity, and the leveling-off is clearly observed in SCF CO_2 (see Figure 5). These results suggest that the fluorescence quenching of DMEA by oxygen competes with but is significantly smaller than the diffusion rate in the lower solvent viscosity range.

For DMEA/CBr_4, as seen in Figure 6, the plot of ln k_q against ln η shows slightly downward curvature in *n*-hexane as observed for DMEA/O_2 in *n*-alkanes; the mean value of β was 0.83 ± 0.02 in the whole pressure range examined and 0.93 ± 0.04 at

TABLE 1: Activation Volumes (cm^3/mol) for k_q, $\Delta V_q^{\ddagger}$, and the Solvent Viscosity, η, $\Delta V_\eta^{\ddagger}$

	DMEA/O_2			DMEA/CBr_4		
	liq CO_2[a]	*n*-hexane[b]	SCF CO_2[c]	liq CO_2[a]	*n*-hexane[b]	SCF CO_2[c]
$\Delta V_q^{\ddagger}$	8 ± 1	11.1 ± 0.2[d]	10 ± 3	42 ± 7	14.1 ± 0.8	400 ± 90
$\Delta V_\eta^{\ddagger}$	79 ± 9	23 ± 1	700 ± 70	79 ± 9	23 ± 1	700 ± 70

[a] At 10 MPa and 25 °C. [b] At 0.1 MPa and 25 °C. [c] At 8.5 MPa and 35 °C. [d] Reference 6.

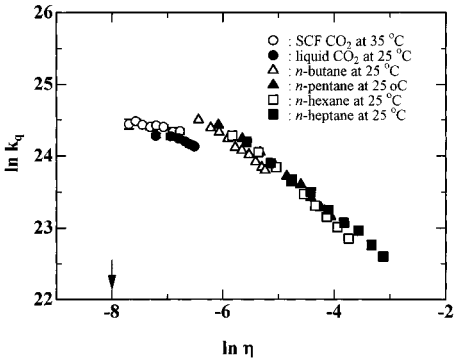

Figure 5. Plots of ln k_q against ln η for DMEA/O_2 in SCF CO_2 at 35 °C, and in liquid CO_2 and *n*-alkanes at 25 °C. The arrow indicates the value of ln η at the critical density and 35 °C.

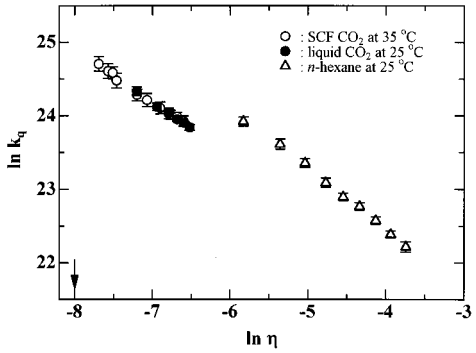

Figure 6. Plots of ln k_q against ln η for DMEA/CBr_4 in SCF CO_2 at 35 °C, and in liquid CO_2 and *n*-alkanes at 25 °C. The arrow indicates the value of ln η at the critical critical density and 35 °C.

pressures above 300 MPa. In liquid and SCF CO_2, the plot of ln k_q against ln η is almost linear (see Figure 6) and the values of β were 0.84 ± 0.04 (SCF CO_2) and 0.71 ± 0.02 (liquid CO_2). Thus, the value of β for DMEA/CBr_4 is close to unity compared to that for DMEA/O_2. From the results, together with the findings for DMEA/O_2, it may be concluded that the fluorescence quenching of DMEA by oxygen competes with diffusion in the whole pressure range examined and probably is only slightly slower than the diffusion rate in the lower viscosity range.

Discussion

Rate Constant for Diffusion, k_{diff}. In general, when the transient terms can be neglected, the rate constant, k_{diff}, for the bimolecular diffusion-controlled reaction between the S_1 state of M, ^{1}M*, and quencher, Q, is given by eq 5 in a solvent with the relative diffusion coefficient, D_{M^*Q} ($=D_{M^*} + D_Q$):[7,8]

$$k_{diff} = 4\pi r_{M^*Q} D_{M^*Q} N_A / 10^3 \quad (5)$$

where r_{M^*Q} and N_A are the encounter distance and Avogadro's number, respectively. The relationship between D_i (i = M* or Q) and ζ_i, the friction coefficient, for the solute molecule, i, in a given solvent is expressed by the Einstein equation, $D_i = k_B T/\zeta_i$, where k_B is the Boltzmann constant. Since the hydrodynamic friction, ζ_i^H, for a solute molecule of spherical radius, r_i, in a continuum medium with viscosity, η, is given by $\zeta_i^H = f_i \pi r_i \eta$ (Stokes' law), one can obtain the Stokes−Einstein (SE) equation

$$D_i^{SE} = k_B T/f_i \pi r_i \eta \quad (6)$$

where $f_i = 4$ and 6 for the slip and stick boundary limits, respectively. However, the SE equation has been often observed to break down for diffusion in liquid and SCF solutions.[7,27−29]

In the previous publications,[19,30,31] the solvent−viscosity dependence of k_{diff} induced by pressure was described successfully for several quenching systems on the basis of an empirical equation proposed by Spernol and Wirtz.[2,32,33] According to their approach, the diffusion coefficient, D_i^{SW}, is expressed by

$$D_i^{SW} = k_B T/6\pi f_i^{SW} r_i \eta \quad (7)$$

where f_i^{SW} represents a microfriction factor and is given by

$$f_i^{SW} = (0.16 + 0.4 r_i/r_S)/(0.9 + 0.4 T_S^r - 0.25 T_i^r) \quad (8)$$

In eq 8, the first parenthetical quantity depends only on the solute-to-solvent size ratio (r_i/r_S). The second parenthetical quantity involves the reduced temperatures, T_S^r and T_i^r, of solvent and solute, respectively, which can be calculated by using the melting point, T_{mp}, and boiling point, T_{bp}, of the solvent or solute at the experimental temperature, T, according to

$$T_{iS}^r = [T - T_{mp(S)}]/[T_{bp(S)} - T_{mp(S)}] \quad (9)$$

From the approximation by Spernorl and Wirtz, eq 10 can be derived

$$k_{diff} = \frac{2RTr_{M^*Q}}{3000\eta}\left(\frac{1}{f_{M^*}^{SW} r_{M^*}} + \frac{1}{f_Q^{SW} r_Q}\right)^{-1} \quad (10)$$

By comparing with eq 1, α^{SW} is given by

$$\alpha^{SW} = \frac{1.2 \times 10^4}{r_{M^*Q}}\left(\frac{1}{f_{M^*}^{SW} r_{M^*}} + \frac{1}{f_Q^{SW} r_Q}\right)^{-1} \quad (11)$$

The values of f_i^{SW}(full) and f_i^{SW}(trunc) can be evaluated by eq 8 and by neglecting the second parenthetical quantity in eq 8, respectively.[2] In this study, we evaluated f_i^{SW}(trunc) alone since f_i^{SW}(full) for the oxygen−solvent systems gives a negative value. In the calculation of f_i^{SW}(trunc), the values of the radii, r_w, of the solute and solvent molecules listed in Table 2 were used. The values of α^{SW}(trunc) thus calculated by eq 11 for the quenching systems studied in this work are shown in Table 2. It is noted in Table 2 that α^{SW}(trunc) are close to the value for slip boundary limit ($\alpha = 2000$) for DMEA/CBr_4 in *n*-hexane and CO_2. However, for DMEA/O_2, α^{SW}(trunc) is significantly smaller than the value for the slip boundary limit; it seems to decrease with decreasing radius of the solvent molecule. This may be attributed to the large difference in the size of DMEA and O_2 as predicted by the first parenthetical quantity in eq 8.

TABLE 2: Values of van der Waals Radii, r_W, of the Solvents and α^{SW}(trunc)

		α^{SW}(trunc)	
	r_W[a]/nm	DMEA/O_2	DMEA/CBr_4
CO_2	0.200	1540	2360
n-butane	0.267	1263	1890
n-pentane	0.285	1211	1800
n-hexane	0.301	1171	1730
n-heptane	0.315	1137	1670

[a] Estimated by the method of Bondi.[34] The values of r_W were evaluated to be 0.173, 0.289, and 0.365 nm for O_2, CBr_4, and DMEA, respectively.

Quenching in Liquid Solution. In the present work, we measured the pressure dependence of the fluorescence quenching constant, k_q, for DMEA/O_2 and DMEA/CBr_4 in both liquid and SCF CO_2, and also that for DMEA/CBr_4 in *n*-hexane. In this section, we first discuss the contribution of diffusion to the quenching for DMEA/O_2 and DMEA/CBr_4 in liquid solution by comparing the result for DMEA/CBr_4 with that for DMEA/O_2 reported previously.[6] Then, we discuss the results obtained in SCF CO_2.

For the fluorescence quenching by heavy-atom quencher (Q) of pyrene (^{1}M*) in liquid solution, the quenching occurs via an exciplex (MQ)* which is formed from an encounter complex $(^1M^*Q)_{en}$ between ^{1}M* and Q in the solvent cage as in Scheme 1,[19] where the bar indicates the solvent cage. Although there is no evidence of the exciplex formation between oxygen and the S_1 state of DMEA, Scheme 1 also may be applied to the present systems under considerations since both of the quenching systems should be kinetically interpreted in the same

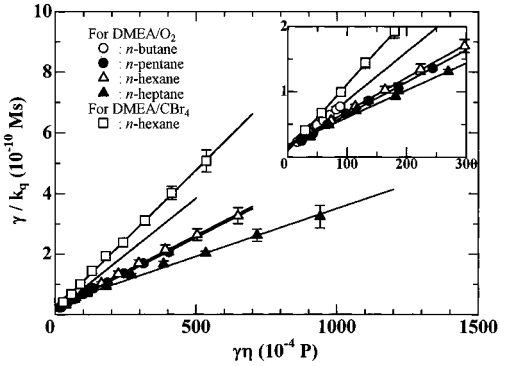

Figure 7. Plots of γ/k_q against $\gamma\eta$ for DMEA/O_2 in *n*-alkane, and for DMEA/CBr_4 in *n*-hexane at 25 °C.

SCHEME 1

$$^1M^* + Q \underset{k_{-diff}}{\overset{k_{diff}}{\rightleftharpoons}} (^1M^*Q)_{en} \underset{k_{-c}}{\overset{k_c}{\rightleftharpoons}} (MQ)^*$$

$$\downarrow k_M \qquad\qquad \downarrow k_p$$

$$^1M + h\nu_M, {}^1M, {}^3M^* \qquad\qquad {}^1M, {}^3M^*$$

framework. Based on Scheme 1, the observed rate constant, k_q, is given by

$$k_q = \frac{k_{-diff}}{1 + k_{-diff}\left(\frac{k_p + k_{-c}}{k_c k_p}\right)} \tag{12}$$

When the rate constant for diffusion, k_{diff}, is expressed by eq 1 (α is replaced by α^{ex}), one may derive eq 13 from eqs 1 and 12.

$$\frac{1}{k_q} = \left(\frac{k_p + k_{-c}}{k_c k_p}\right)\left(\frac{k_{-diff}}{k_{diff}}\right) + \frac{\alpha^{ex}}{8RT}\eta \tag{13}$$

In eq 13, the pressure dependence of k_{diff}/k_{-diff} is assumed to be given by that of the radial distribution function, $g(r_{M^*Q})$, at the closest approach distance (the encounter distance), r_{M^*Q} ($=r_{M^*} + r_Q$) with hard spheres.[19] By using this relation, eq 14 is derived and successfully applied to the fluorescence quenching by the heavy-atom quenchers with a nearly diffusion-controlled rate.[19]

$$\frac{\gamma}{k_q} = \left(\frac{k_p + k_{-c}}{k_c k_p}\right)\left(\frac{k_{-diff}}{k_{diff}}\right)_0 + \frac{\alpha^{ex}}{8RT}\gamma\eta \tag{14}$$

where γ is the ratio of $g(r_{M^*Q})$ at P MPa to that at a reference pressure, P_0 MPa, $g(r_{M^*Q})_P/g(r_{M^*Q})_0$, and $(k_{-diff}/k_{diff})_0$ is k_{-diff}/k_{diff} at P_0 MPa.[35] According to eq 14, the plot of γ/k_q against $\gamma\eta$ should be linear when $(k_p + k_{-c})/(k_c k_p)$ is independent of pressure.

The plot of γ/k_q against $\gamma\eta$ for DMEA/O_2 in *n*-alkanes (C_4 to C_7) and also for DMEA/CBr_4 in *n*-hexane is shown in Figure 7. The plot of γ/k_q against $\gamma\eta$ for DMEA/O_2 and DMEA/CBr_4 in liquid CO_2 is also shown in Figure 8a. All the plots shown in Figures 7 and 8a are approximately linear with positive intercepts, indicating that the quenching competes with diffusion, and hence $(k_p + k_{-c})/k_c k_p$ is approximately independent of $\eta\gamma$, that is, pressure. These observations are consistent with those found for the fluorescence quenching by polybromomethanes

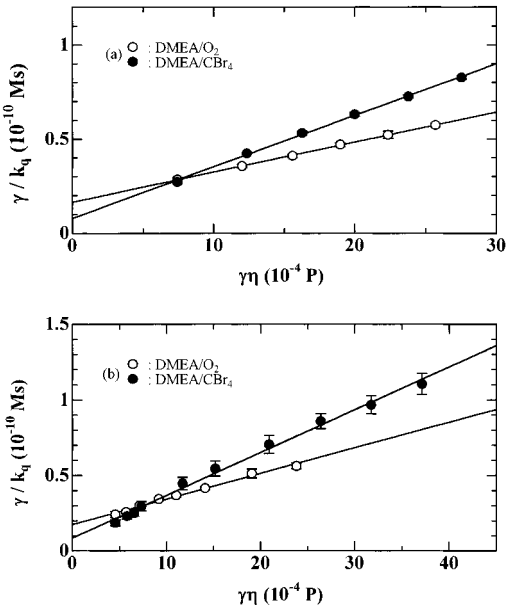

Figure 8. Plots of γ/k_q against $\gamma\eta$ for DMEA/O_2 and DMEA/CBr_4 in (a) liquid CO_2 at 25 °C and (b) SCF CO_2 at 35 °C.

TABLE 3: Values of α^{ex} and $k_{bim}{}^0$ for DMEA/O_2 in SCF CO_2 at 35 °C, and in Liquid CO_2 and *n*-Alkanes at 25 °C

	DMEA/O_2		DMEA/CBr_4	
solvent	α^{ex}	$k_{bim}{}^0/10^{10}$ M^{-1} s^{-1}	α^{ex}	$k_{bim}{}^0/10^{10}$ M^{-1} s^{-1}
SCF CO_2	3500 ± 300	5.7 ± 0.9[a]	5800 ± 200	12 ± 4[a]
liquid CO_2	3100 ± 100	6.0 ± 0.2[b]	5200 ± 200	12 ± 2[b]
n-butane	1480 ± 30	8.5 ± 0.7[c]		
n-pentane	940 ± 20	5.6 ± 0.9[d]		
n-hexane	940 ± 20	5.4 ± 0.8[d]	1820 ± 30	5.5 ± 0.9[d]
n-heptane	690 ± 40	3.6 ± 0.9[d]		

[a] At 8.5 MPa and 35 °C. [b] At 10 MPa and 25 °C. [c] At 3.0 MPa and 25 °C. [d] At 0.1 MPa and 25 °C.

of pyrene in methylcyclohexane.[19] The values of α^{ex} and the bimolecular rate constant, $k_{bim}{}^0$, defined by eq 15

$$k_{bim}{}^0 = \left(\frac{k_p k_c}{k_p + k_{-c}}\right)\left(\frac{k_{-diff}}{k_{diff}}\right) \tag{15}$$

were determined from the least-squares intercept and slope of the plots (Figures 7 and 8) and are summarized in Table 3. For DMEA/O_2, α^{ex} is nearly equal to α^{SW}(trunc) in *n*-butane, *n*-pentane, and *n*-hexane, whereas it is significantly larger than that in liquid CO_2. For DMEA/CBr_4, α^{ex} is nearly equal to α^{SW}(trunc) in *n*-hexane, but one can also see large discrepancy between α^{ex} and α^{SW}(trunc) in liquid CO_2 as found for DMEA/O_2.

In the previous work,[19,30,31] we showed that α^{ex} is well described by α^{SW} for the heavy-atom quenching of fluorescence of pyrene in liquid solution. In this work, α^{SW}(trunc) also gives good approximation to α^{ex} for DMEA/CBr_4 in *n*-hexane and for DMEA/O_2 in *n*-alkanes (C_4 to C_6) except for *n*-heptane. However, α^{ex} is about 2 times larger than α^{SW}(trunc) in liquid CO_2 for both of the quenching systems. The microfriction factor, f_i^{SW} given by eq 8 involves the solute−solvent interactions as well as the solute-to-solvent size ratio. Hence, it seems likely that the expression of f_i^{SW} (eq 8) cannot be applied for DMEA/O_2 and DMEA/CBr_4 in liquid CO_2. That is, for these systems, larger f_i^{SW} (i = DMEA, O_2, and CBr_4), which may arise as results of stronger solute−solvent interactions and/or larger

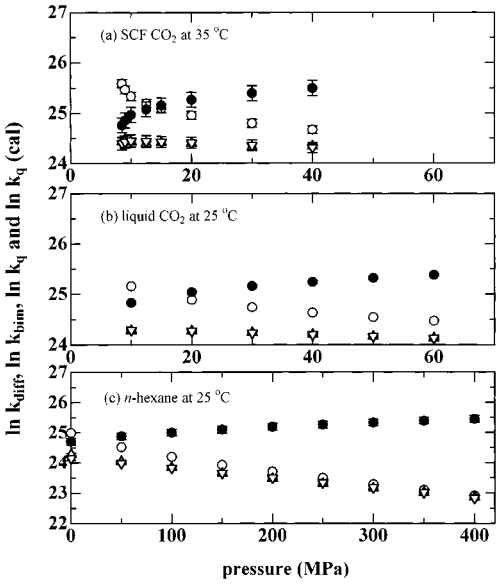

Figure 9. Pressure dependence of k_{diff} (○), k_{bim}(●), k_q (△), and k_q(cal) (▽) for DMEA/O_2 in (a) SCF CO_2 at 35 °C, (b) liquid CO_2, and (c) *n*-hexane at 25 °C.

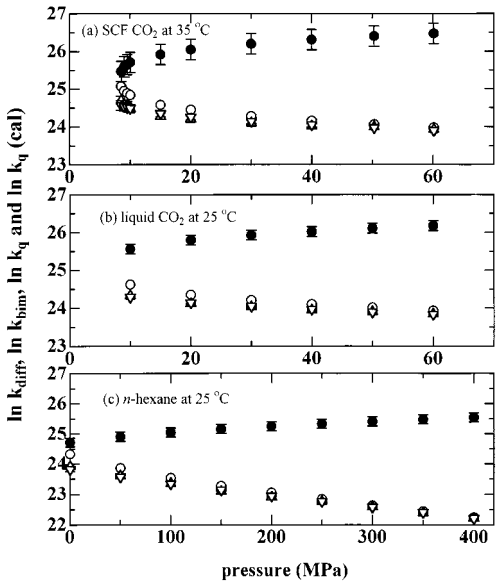

Figure 10. Pressure dependence of k_{diff} (○), k_{bim}(●), k_q (△), and k_q(cal) (▽) for DMEA/CBr_4 in (a) SCF CO_2 at 35 °C, (b) liquid CO_2, and (c) *n*-hexane at 25 °C.

contribution of the solute−solvent size ratio as compared to those predicted by eq 8, might be expected although the $1/\eta$ dependence of k_{diff} is still valid.

Quenching in SCF CO_2. The plot of γ/kq against $\gamma\eta$ for DMEA/O_2 and DMEA/CBr_4 in SCF CO_2 is shown in Figure 8b. The plots shown in Figure 8b are approximately linear with positive intercepts, meaning that the quenching competes with diffusion and hence $(k_p + k_{-c})/k_c k_p$ is approximately independent of $\gamma\eta$, that is, pressure. These observations are consistent with those found in liquid solutions described in the previous section. The values of α^{ex} and the bimolecular rate constant, k_{bim}^0 (eq 15), which were determined from the least-squares slope and intercept of the plots shown in Figure 8b, respectively, are listed in Table 3, together with those in liquid solutions. It is noted in Table 3 that the values of k_{bim}^0 in SCF CO_2 (35 °C, 8.5 MPa) are approximately equal to those in liquid CO_2 (25 °C, 10.0 MPa) for DMEA/O_2 and DMEA/CBr_4, respectively. It is also noted that the value of α^{ex} in SCF CO_2 is approximately equal to that in liquid CO_2 for DMEA/O_2 and DMEA/CBr_4, respectively. The latter fact indicates that the rate constant for diffusion, k_{diff}, depends only on solvent viscosity, η, suggesting that the quenching in SCF CO_2 can be interpreted in terms of the same framework as the Scheme 1 with the solvent cage effect.

Pressure Dependence of k_{bim} and the Contribution of Diffusion to the Quenching. The values of k_{bim} can be calculated by $k_{bim} = k_{bim}^0\gamma$, and those of k_{diff} also reproduced using α^{ex} (Table 3) and the solvent viscosity, η, according to eq 1. By using the values of k_{bim} and k_{diff}, k_q(cal) is calculated by eq 16 (see eq 13).

$$k_q(\text{cal}) = \frac{k_{bim}k_{diff}}{k_{bim} + k_{diff}} \tag{16}$$

The pressure dependences of k_{bim}, k_{diff}, k_q, and k_q(cal) thus calculated are shown in Figures 9 and 10 for DMEA/O_2 and DMEA/CBr_4, respectively. For DMEA/O_2 in SCF CO_2 (Figure 9a), k_{diff} is significantly larger than k_{bim} at pressures of 8.5 and 9.0 MPa, then close together, and their difference increases as pressure increases further. In liquid CO_2 and *n*-hexane (Figure 9, b and c), k_{diff} is close to k_{bim} at the lower pressure range and their difference increases with increasing pressure. These results indicate that the contribution of diffusion to the quenching is significant in both liquid and SCF CO_2 in the pressure range examined.

For DMEA/CBr_4, one can find similar observations as seen in Figure 10, but the difference between k_{diff} and k_{bim} is larger when compared to that for DMEA/O_2. Therefore, the contribution of diffusion to the quenching is significant even in the lower pressure region. As a result, for both the systems of DMEA/O_2 and DMEA/CBr_4, the quenching approaches the diffusion-controlled rate in the higher pressure region since k_{diff} decreases whereas k_{bim} increases with increasing pressure.

Summary

It has been demonstrated that the fluorescence quenching by oxygen of 9,10-dimethylanthracene (DMEA) is not fully diffusion-controlled but competes with diffusion in the solvents with low viscosity by comparing the pressure and the pressure-induced solvent viscosity dependence of DMEA/O_2 and DMEA/CBr_4. The analysis by eq 14 clearly reveals the contribution of diffusion to the quenching in DMEA/CBr_4 as well as in DMEA/O_2. The bimolecular rate constants for the quenching, k_{bim}, which increases with increasing the radial distribution function at the closest approach distance with the hard-sphere assumption, are found to be ca. 6×10^{10} and 1.2×10^{11} M^{-1} s^{-1} for DMEA/O_2 and DMEA/CBr_4, respectively, in both liquid CO_2 (25 °C, 10 MPa) and SCF CO_2 (35 °C, 8.5 MPa.). It has been shown that the observed quenching constant, k_q, is given by eq 16 using k_{bim} and k_{diff}. The latter is inversely proportional to the solvent viscosity, η (eq 1).

References and Notes

(1) Birks, J. B. *Photophysics of Aromatic Molecules*; Wiley-Interscience: New York, 1970; p 518.

(2) Saltiel, J.; Atwater, B. W. *Advances in Photochemistry*; Wiley-Interscience: New York, 1987; Vol. 14, p 1.

(3) Ware, W. R. *J. Phys. Chem.* **1962**, *66*, 455.

(4) Yasuda, H.; Scully, A. D.; Hirayama, S.; Okamoto, M.; Tanaka, F. *J. Am. Chem. Soc.* **1990**, *112*, 6847.

(5) Hirayama, S.; Yasuda, H.; Scully, A. D.; Okamoto, M. *J. Phys. Chem.* **1994**, *98*, 4609 and references therein.

(6) Okamoto, M.; Tanaka, F.; Hirayama, S. *J. Phys. Chem.* **1998**, *102*, 10703.

(7) Birks, J. B. *Organic Molecular Photophysics*; Wiley: New York, 1973; p 403.
(8) Rice, S. A. In *Comprehensive Chemical Kinetics. Diffusion-Limited Reactions*; Bamford, C. H., Tripper, C. F. H., Compton, R. G., Eds.; Elsevier: Amsterdam, 1985; Vol. 25.
(9) As a review article: Kajimoto, O. *Chem. Rev.* **1999**, *99*, 355.
(10) Brennecke, J. F.; Tomasko, D. L.; Eckert, C. *J. Phys. Chem.* **1990**, *94*, 4, 7692.
(11) Zagrobelny, J.; Betts, T. A.; Bright, F. V. *J. Am. Chem. Soc.* **1992**, *114*, 5249.
(12) Randolph, T. W.; Carlier, C. *J. Phys. Chem.* **1992**, *96*, 5146.
(13) Zagrobelny, J.; Bright, F. V. *J. Am. Chem. Soc.* **1993**, *115*, 701.
(14) Roberts, C. B.; Zhang, J.; Brennecke, J. F.; Chateauneuf, J. E. *J. Phys. Chem.* **1993**, *97*, 5618.
(15) Worrall, D. R.; Wilkinson, F. *J. Chem. Soc., Faraday Trans.* **1996**, 92, 1467.
(16) Bunker, C. E.; Sun Y.-P. *J. Am. Chem. Soc.* **1995**, *117*, 10865.
(17) Bunker, C. E.; Sun, Y.-P. *J. Phys. Chem. A* **1997**, *101*, 9233.
(18) Zhang, J.; Rock, D. P.; Chateauneuf, J. E.; Brennecke, J. F. *J. Am. Chem. Soc.* **1997**, *119*, 9980.
(19) Okamoto, M. *J. Phys. Chem. A* **2000**, *104*, 7518.
(20) Okamoto, M.; Teranishi, H. *J. Phys. Chem.* **1984**, *88*, 5644.
(21) Brazier, D. W.; Freeman, G, R. *Can. J. Chem.* **1969**, *47*, 893.
(22) Herreman, W.; Grevendonk, W.; Bock, A. De *J. Chem. Phys.* **1970**, *53*, 19.
(23) Iwasaki, H.; Takahashi, M. *J. Chem. Phys.* **1981**, *74*, 1930.
(24) Diller, D. E.; Ball, M. J. *Inter. J. Thermophys.* **1985**, *6*, 619.
(25) Lamb, D. M.; Adamy, S. T.; Woo, K. W.; Jonas, J. *J. Phys. Chem.* **1989**, *93*, 5002.
(26) van der Gulik P. S.; Mostert, R.; van den Berg, H. R. *High-Temp. High-Press.* **1991**, *23*, 87.
(27) Evance, D. F.; Tominaga, T.; Chan, C. *J. Soln. Chem.* **1979**, *8*, 461.
(28) Evance, D. F.; Tominaga, T.; Davis, H. T. *J. Chem. Phys.* **1981**, *74*, 1298.
(29) As a review article: Funazukuri, T. *Rev. High-Press. Sci. Technol.* **1996**, *5*, 34.
(30) Okamoto, M. J. *Phys. Chem. A* **1998**, *102*, 4751.
(31) Okamoto, M. J. *Phys. Chem. A* **2000**, *104*, 5029.
(32) Spernol, A.; Wirtz, K. Z. *Naturforsch.* **1953**, *8A*, 522.
(33) Gierer, A.; Wirtz, K. Z. *Naturforsch.* **1953**, *8A*, 532.
(34) Bondi, A. *J. Phys. Chem.* **1964**, *68*, 441.
(35) The radial distribution function at the closest approach distance, r_{M^*Q} ($=r_{M^*} + r_Q$) with the hard-sphere assumption, $g(r_{M^*Q})$ is given by[36] eq A-1
(36)

$$g(r_{M^*Q}) = \frac{1}{1-y} + \frac{3y}{(1-y)^2}\left(\frac{r_{red}}{r_S}\right) + \frac{2y^2}{(1-y)^3}\left(\frac{r_{red}}{r_S}\right)^2 \qquad \text{(A-1)}$$

where $r_{red} = r_{M^*}r_Q/r_{M^*Q}$, and y is the packing fraction, given in terms of the molar volume of solvent, V_S, by eq A-2

$$y = \frac{4N_A\pi r_S^{\,3}}{3V_S} \qquad \text{(A-2)}$$

By using the values of r_S, r_{M^*}, and r_Q listed in Table 2, together with the data of the solvent density,[21−26] $g(r_{M^*Q})$ was calculated by (A-1).
(37) Yoshimura, Y.; Nakahara, M. *J. Chem. Phys.* **1984**, *81*, 4080.